**The role of the angle of the fibularis longus tendon in foot arch support**

Anoop S. Sumal[1*], Gavin E. Jarvis[1], Alan R. Norrish[2], Cecilia Brassett[1] and Robert H. Whitaker[1]

[1]Human Anatomy Teaching Group, Department of Physiology, Development & Neuroscience, University of Cambridge, Cambridge, UK, CB2 3DY

[2]Research Fellow in Academic Orthopaedics, Trauma and Sports Medicine, School of Medicine, University of Nottingham, Nottingham, UK

**Abbreviated title**: Fibularis longus and arch support

**Corresponding author**: Mr. Anoop S. Sumal, Human Anatomy Teaching Group, Department of Physiology, Development & Neuroscience, University of Cambridge, Downing site, CB2 3DY. Email: as2557@cam.ac.uk.

Research was presented at the British Association of Clinical Anatomy (BACA) Winter Meeting on 17th December 2019 at Newcastle Medical School, Newcastle University, NE2 4HH, UK. Abstract is to be published in their journal, Clinical Anatomy.

**Author's contributions**

A.S.S., R.H.W. and C.B. created concept for the project and interpreted data. A.S.S. carried out methodology, wrote original draft and complied feedback from all authors. R.H.W created figures 1-3. R.H.W. and C.B. enabled project and provided equipment. A.S.S. and G.E.J. performed statistical analysis. A.S.S., R.H.W., C.B., G.E.J. and A.R.N. revised drafts and assisted in editing of manuscript. All authors have read and approved the final submitted manuscript.

**Acknowledgements**

We thank the donors for allowing cadaveric research to be possible. Thanks to Professor Michael Sutcliffe, Department of Engineering, University of Cambridge, for recommending the Capstan equation. To the Human Dissection Room technical staff for their general support and providing the necessary equipment.

# The role of the angle of the fibularis longus tendon in foot arch support


## Abstract

**Introduction**: Understanding the contribution of the fibularis longus tendon to the support of the midfoot arches has potential therapeutic applications. This cadaveric study sought to quantify this support across both the transverse arch and medial longitudinal arch and to establish whether a correlation exists between this support and the angle at which the tendon enters the sole.

**Materials and Methods**: Markers placed in 11 dissected cadaveric foot specimens defined the arch boundaries. Incremental weights up to 150 N were applied to the fibularis longus tendon to simulate progressive muscle contraction, and associated changes in the transverse and medial longitudinal arch boundaries were recorded.

**Results**: A force of 150 N reduced the transverse arch distance by 4.6 (1.7) mm (mean (SD)) and medial longitudinal arch distance by 6.8 (1.4) mm. The angle of the fibularis longus tendon on the sole correlated well with changes in the transverse arch distance (slope ± s.e. = 0.56 ± 0.13 mm.degree$^{-1}$, Pearson $r = 0.83$, $p = 0.002$) but only weakly with the medial longitudinal arch (0.18 ± 0.18 mm.degree$^{-1}$, $r = 0.32$, $p = 0.33$).

**Conclusions**: The results of this preliminary study raise the possibility that physical therapies targeting the fibularis longus tendon may be valuable in the management of midfoot arch collapse. The correlation observed with the transverse arch suggests the possibility that surgical

modification of the angle of the fibularis longus tendon on the sole may benefit patients with transverse arch collapse.

**Keywords:** anatomy; foot arches; fibularis longus; cadaveric study; arch collapse.

**Abbreviations**

Angle of fibularis longus tendon on sole, $\theta$

Acquired flat foot deformity, AFFD

Fibularis longus, FL

Medial longitudinal arch, MLA

Transverse foot arch, TFA

## Introduction

The foot arches play very important roles. Their functions include providing stability to support the body weight, contributing to the mechanism of gait, and protecting the articular surfaces of the joints of the lower limb (Birinci and Demirbas, 2017).

Loss of the normal arches, in particular the medial longitudinal arch (MLA), is implicated in a number of important clinical conditions such as acquired *pes planus*. It is thought to occur in 20-30% of the population to some degree, and may often be an asymptomatic physiological variant in some individuals (Raj et al., 2019). However, *pes planus* may be associated with symptoms such as pain on walking, and corresponding tendinitis of the long tendons which pass under the collapsed foot arches secondary to abnormal excursion. *Pes planus* is commonly caused by rupture of the plantar aponeurosis (Standring 2005), and is often observed in women over the age of 40 due to natural tibialis posterior degeneration (Kohls-Gatzoulis et al., 2004). However, loss or weakness of any muscle supporting the arches may also result in this condition.

The tendons passing deep to the sole of the foot are important in maintaining the normal foot arches. Amongst these, the fibularis longus (FL) tendon is unique. The FL muscle lies in the lateral compartment of the leg, and forms a tendon that passes posterior to the lateral malleolus. It then courses into the sole of the foot, deep to the long plantar ligament, to cross the sole obliquely (Figs. 1a-b). The tendon inserts onto the lateral aspects of the bases of the first metatarsal and medial cuneiform (Standring, 2005). Variations in its insertion have been noted, including slips onto the bases of the second and fifth metatarsals or a wide insertion across the base of the first metatarsal (Gomes et al., 2019). The FL primarily acts to plantarflex the ankle and first tarsometatarsal joints, as well as everting the foot at the midtarsal and subtalar joints.

The FL tendon is an extrinsic tendon that crosses the sole obliquely, generating tension across the joints of both transverse and longitudinal arches. Its oblique nature creates an angle between the FL tendon and the midline of the foot, which is referred to throughout as the angle of the FL tendon on the sole (θ), which may alter the support provided by FL to the transverse foot arch (TFA) and the MLA (Fig. 1b). While some evidence exists to suggest that the oblique passage of the FL tendon across the sole assists in supporting the midfoot arches (Standring, 2005), it is often limited and the effects of the θ has not been extensively explored.

This preliminary cadaveric study aims to identify whether simulated FL tendon contraction acts to support the MLA and the TFA, and to quantify any effect that the θ has on this support.

## Materials and Methods

*Specimen preparation*

Eleven human cadaveric specimens of the lower leg and foot (distal to the midpoint of the tibia) were provided by Human Dissection Room, Anatomy Building, Department of Physiology, Development and Neuroscience, University of Cambridge, UK. The donors (5 male, 6 female; mean (SD) age = 78.5 (12.5) years, Table 1) had provided consent for anatomical research prior to decease in compliance with the Human Tissue Act 2004 and were embalmed using a vascular technique (with a solution of water, ethanol, formaldehyde and menthol). None of the donors had undergone previous foot surgery or had any recorded foot pathologies. The foot specimens were dissected to a deep level, defined as removal of skin and fascia of the sole, all intrinsic plantar foot muscles, soft tissue from the dorsum of the foot and all long tendons except for the FL tendon. The FL tendon was sectioned proximal to the lateral malleolus and pretensioned with weights prior to testing. All specimens were stored at the same temperature (20 °C).

*Markers*

Markers (pins) were inserted on the sole of each specimen to uniformly identify the MLA and the TFA (Fig. 1c-d). They were defined as the: (A) midpoint of the calcaneus on the inferior surface along the midline of the foot, a fixed point as the calcaneus was clamped; (B) medial aspect of the medial cuneiform, the most medial aspect of the transverse arch, and (C) midpoint of the base of the fifth metatarsal, the most lateral aspect of the transverse arch. The longitudinal distance between markers (A) and (B) represents the MLA and the transverse distance between markers (B) and (C) represents the TFA (Fig. 1c). As the joint between the fifth metatarsal and lateral cuneiform does not form part of the transverse arch, the movement at this joint was minimized by fixing the lateral aspect of the foot against a plastic block during testing.

*Experimental apparatus*

In order to mimic conditions during the mid- to terminal-stance phase of gait, the calcaneus of each specimen was secured by a vice with the ankle dorsiflexed. Each specimen was secured with the sole facing upwards which allowed observation of the markers and a modified vice allowed access to the FL tendon. The sole of the specimen was levelled in the horizontal plane, aligning the metatarsophalangeal joints with the calcaneus as these are the major pressure points on weight-bearing over a wide range of weight-bearing percentages (Jones, 1941; Shelton et al., 2019). By the use of a laser level (Fig. 2), each specimen was aligned into the anatomical position defined by Renton (1991), *i.e.* a line passing from the midpoint of the calcaneus to between the heads of the second and third metatarsals. A camera (iPad) was positioned above the specimens to take scaled photographs of the marker positions, with a ruler included in each photograph, allowing for subsequent analysis of angles and distances.

*Simulating FL contraction*

The proximal end of the sectioned FL tendon was secured to weighing scales, from which a bucket was hung. In addition to the force exerted by the bucket and scales on the FL tendon, a range of 0-150 N (in intervals of 10 N) were applied to the tendon by adding weights to the bucket. This range sought to simulate human physiological FL tendon contraction and was derived from studies demonstrating the peak eversion torque of the human foot (Kaminski et al., 1999; Zhao et al., 2018), and considering the contribution that other evertors of the foot may have, such as fibularis brevis and tertius (Davda et al., 2019).

The directional changes of the FL tendon (at the lateral malleolus and as it crosses on to the sole), along with the frictional coefficient at these bends affect the tension at its insertion. This study standardized the tension at the insertion to the range of 0-150 N by use of the Capstan equation (footnote 1; Fig. 3; Table S-1), which required measurements of the angles at the directional changes and frictional coefficient at the bone-muscle interface. The angle of the (first) directional change at the ankle joint was fixed at 47.5° and the (second) directional change, as the FL tendon crosses onto the sole, was measured to the nearest five degrees. The frictional coefficient was estimated at 0.035 (Uchiyama et al., 1995; Amadio, 2005).

*Measurements*

Scaled photographs of the specimens were taken on each addition of weight and subsequently analyzed using Fiji 2.0.0 to allow for accurate measurements of the θ and arch distances (Schindelin et al., 2012). The AB longitudinal distance and BC transverse distance were measured at each weight interval, whilst the θ was measured at 0 N and assumed to remain constant during testing. The θ was measured from the midline of the foot to a line passing between the midpoints of the FL tendon at its insertion and as it bends onto the sole. Only the sole was visible on the photographs, and the angles of the directional changes of the FL tendon were instead measured using a protractor. All measurements were made by the same observer.

Seven sets of measurements were performed on the first specimen (male, right side, 68 years) to refine methodology and establish reproducibility. Two out of these seven measurement sets used the same protocol subsequently used for the remaining specimens and generated values for the predicted distance change provided by a force of 150 N ($\Delta_{dist150}$) as follows: for the TFA, 2.9 and 3.2 mm (coefficient of variance, CV = 6.0%); for the MLA, 7.3 and 7.4 mm (CV = 1.5%). This reproducibility and the observation that repeated measurements gradually damaged the specimens led us to decide that two replicates per specimen was an optimal practical design for the remaining specimens.

*Statistical analysis*

Having measured the arch distances at 0-150 N on two separate occasions, the values were averaged and the force-arch (or AB and BC) distance relationships of each specimen were modelled using the following equation: $\mathbf{y_F = (y_0 - B).e^{-kx} + B}$, where: $y_F$ = predicted distance when force = x, x = force applied, $y_0$ = predicted distance when x = 0, B = asymptotic baseline distance when x = ∞, k = a force constant that defines the relationship between force and distance (Fig. 4). The parameters $y_0$, B and k were estimated using a least squares minimization approach (Table 1), and were used to plot the modelled line allowing comparisons of the arch distance changes across all specimens. The predicted change in distance caused by a force of 150 N ($\Delta_{dist150}$) was calculated for each specimen as $\Delta_{dist150} = y_0 - y_{150}$ (Table 1). Simple linear regression ($r$) was performed on the θ and $\Delta_{dist150}$ for both arches, and the statistical significance of each correlation was determined. The significance level was $p < 0.05$.

## **Results**

Measurements were obtained from 11 specimens. The angle of the FL tendon on the sole (θ, mean (SD)) was 37.7 (2.5) degrees. A force of 150 N caused a decrease in transverse foot arch (TFA) distance ($\Delta_{dist150}$) of 4.6 (1.7) mm and in the medial longitudinal arch (MLA) of 6.8 (1.4) mm. $\Delta_{dist150}$ was positively correlated with θ. For TFA, this effect was strong: for each degree change in angle, $\Delta_{dist150}$ decreased by 0.56 ± 0.13 mm.degree$^{-1}$ (mean ± s.e.; $r = 0.83$, $p = 0.002$). Across the MLA, however, this effect was weak (0.18 ± 0.18 mm.degree$^{-1}$, $r = 0.32$, $p = 0.33$). Figure 5 shows the correlation between the θ and $\Delta_{dist150}$ of both the TFA and the MLA. Tables S-2 and S-3 show the observed TFA and MLA distance changes at each force, respectively.

## **Discussion**

During gait, the action of FL is to stabilize the medial aspect of the foot and prevent extreme inversion (Moore et al., 2014), aiding its function of responding to sudden inversion of the foot (Konradsen et al., 1997). Therefore, the FL tendon may have an important role in stabilizing the foot arches. Bojsen-Moller (1979) described that when the foot joints are loosely packed, they are unstable and to this extent are unsupported; however, when the foot joints become tightly packed, they are supported. It is through this mechanism, by increasing the tension and apposition between the midfoot joints, that the FL tendon contributes to the maintenance of the normal foot arches.

In this study, simulated FL tendon contraction in cadaveric specimens decreased the TFA and MLA arch distances confirming that the tendon supports both arches. The arch distance changes decreased with higher forces, most likely because the joints comprising the arches had reached the limits of their movements.

*Fibularis longus & medial longitudinal arch*

The role of FL in supporting the MLA is controversial. It has been noted that the function of FL in raising the MLA is negligible mainly because the moment it produces across the joint between the first metatarsal and medial cuneiform is small compared to other leg muscles such as tibialis posterior (Angin et al., 2014), and a cadaveric study has questioned the importance of this tendon in providing support to the MLA during the stance phase of gait (Dullaert et al., 2016). In addition, Sharkey et al. (1998) have shown no significant role of FL in supporting the foot arches at the end of the stance phase, and instead argued that the plantar aponeurosis is the key supporter of the arches. The plantar aponeurosis is thought to support the foot arches through the Windlass Mechanism and provides stiffness to the foot during locomotion (Hicks, 1954; Bolgla and Malone, 2004). Conversely, Fessel et al. (2014) have shown that this aponeurosis remains completely relaxed during gait, and the dynamic supports are the key arch supporters. These studies highlight the controversy surrounding the most crucial foot arch supporters.

Other studies suggest that the FL tendon supports the MLA. Thordarson et al. (1995) showed that the FL tendon provides deforming forces to the MLA during the stance phase of gait, and its contraction causes locking of the first metatarsal ray and thus provides stabilization to the MLA (Johnson and Christensen, 1999; Bierman et al., 2001). Electromyographic studies also confirm its role in MLA support during the stance phase of gait, as the activity of FL is reduced in patients with *pes planus* compared to patients with normal arches (Hunt and Smith, 2004; Murley et al., 2009).

Despite acquired flatfoot deformities (AFFDs) of the MLA often being associated with tibialis posterior or spring ligament defects (Arain et al., 2019), their pathogenesis and subsequently their management remain unclear and controversial (Tao et al., 2019). This study suggests that the FL tendon supports the MLA, and may provide a novel therapeutic target in the management of AFFDs.

*Fibularis longus & transverse arch*

Less controversial is the role of the FL tendon in supporting the TFA, which is also evident in this study. The oblique nature of the FL tendon, *i.e*. more transverse than longitudinal in the sole, preferentially provides support in the transverse plane. The importance of the TFA has been recently highlighted by Venkadesan et al. (2020), as they have shown that it contributes to 40% of the stiffness of the foot, which aids to reduce flatfoot during locomotion. They note that this knowledge may help in the management of flatfoot disorders. Therapeutically targeting the FL tendon in TFA arch collapse could help to ameliorate *pes planus*.

*The angle on the sole*

A significant positive correlation was only observed between the θ and the TFA distance changes ($r = 0.83$, $p = 0.002$). Therefore, the θ may alter the support that the FL tendon provides to the TFA. Increases in the θ results in increases in the TFA distance changes and support provided to this arch by the FL tendon.

Knowledge of the θ allows consideration of novel therapeutic interventions to surgically re-position the FL tendon for maintenance of the TFA *e.g*. in cases of TFA collapse not responsive to muscle training or orthotic support. Basit et al. (2019) indicated that the FL and fibularis brevis tendons are the most commonly dislocated in the ankle, and in these cases, it may be reasonable to surgically re-position and fix the FL tendon in favour of supporting the TFA.

*Limitations*

This study is restricted by a number of limitations, most notably its small sample size. This study used formalin-fixed specimens, known to reduce the range of motion of human joints and have fixing effects on tendons (Balta et al., 2015; Balta et al., 2019). In addition, it been shown that the Young's Modulus (stiffness) of formalin-fixed tendons is significantly higher than of fresh-frozen specimens (Hohmann et al., 2019). Therefore, our study may not offer an ideal representation of the behavior of the FL tendon in non-embalmed cadavers and living subjects, and should be interpreted accordingly. This study was not able to account for the effects of weight-loading which would otherwise act during the stance phase of gait. Loading the specimens with weight would flatten the MLA (Shelton et al., 2019), which would counteract the distance changes observed. By using cadaveric specimens, we were able to isolate the FL tendon, but this was at the expense of losing local surrounding structures such as the plantar aponeurosis. The effects of losing this aponeurosis, however, may have been circumvented as weight-loading was not considered. The lateral aspect of the specimens was fixed using a plastic block, which helped to reduce any misalignment on progressive simulated FL tendon contraction. Loading the FL tendon at 150 N, however, stressed the experimental apparatus and some specimens lost the alignment provided by the laser level. The results of this study should be regarded as preliminary and should be verified with further rigorous testing.

## **Conclusions**

This study provides evidence that the FL tendon has a supportive effect on both the TFA and the MLA, as on its simulated contraction, the distance of both arches reduced. Whilst the effect on the TFA is not controversial, the supportive effect of FL on the MLA is more contentious. This study indeed demonstrates that whilst the effect of FL on the TFA is related to the angle at which the tendon enters the sole, the same does not appear to hold true for the MLA. Targeting the FL tendon may provide a novel physical (or surgical) method in the management of AFFDs. This preliminary study provides a foundation to further investigate this unique tendon and its actions on arch support. Future studies should quantify its effects on the arches in live participants during gait and weight-loading activities, and compare its supportive effect to other key arch supporters, namely tibialis posterior and the plantar aponeurosis.

## **References**


Amadio, P. (2005). Friction of the Gliding Surface. *J Hand Ther, 18*(2), 112-119.

Angin, S., Crofts, G., Mickle, K. and Nester, C. (2014). Ultrasound evaluation of foot muscles and plantar fascia in pes planus. *Gait Posture, 40*(1), 48-52.

Arain, A., Harrington, M.C. and Rosenbaum, A. J. (2019). Adult Acquired Flatfoot (AAFD). URL: https://www.ncbi.nlm.nih.gov/books/NBK542178/?report=reader

Balta, J.Y., Cronin M., Cryan J.F. and O'mahony S.M. (2015). Human preservation techniques in anatomy: A 21st century medical education perspective. *Clin Anat*, *28*(6), 725-734.

Balta, J.Y., Twomey, M., Moloney, F., Duggan, O., Murphy, K.P., O'Connor, O.J., Cronin, M., Cryan, J.F., Maher, M.M. and O'Mahony, S.M. (2019). A comparison of embalming fluids on the structures and properties of tissue in human cadavers. *Anat, Histol Embryol*, *48*(1), pp.64-73.

Basit, H., Eovaldi, B.J. and Siccardi, M.A. (2019). Anatomy, Bony Pelvis and Lower Limb, Foot Peroneus Brevis Muscle. URL: https://www.ncbi.nlm.nih.gov/books/NBK535427/

Bierman, R., Christensen, J. and Johnson, C. (2001). Biomechanics of the first ray. Part III. Consequences of lapidus arthrodesis on peroneus longus function: A three-dimensional kinematic analysis in a cadaver model. *J Foot Ankle Surg, 40*(3), 125-131.

Birinci, T. and Demirbas, S. (2017). Relationship between the mobility of medial longitudinal arch and postural control. *Acta Orthop Traumatol Turc, 51*(3), 233-237.

Bojsen-Moller, F. (1979). Calcaneocuboid joint and stability of the longitudinal arch of the foot at high and low gear push off. *J Anat, 129*(1), 165.

Bolgla, L.A. and Malone, T.R. (2004). Plantar fasciitis and the windlass mechanism: a biomechanical link to clinical practice. *J Athl Train, 39*(1), 77-82.

Davda K., Malhotra K., O'Donnell P., Singh D. and Cullen N. Peroneal tendon disorders. (2017). *EFORT Open Rev, 2*(6), 281-92.

Dullaert, K., Hagen, J., Klos, K., Gueorguiev, B., Lenz, M., Richards, R.G. and Simons, P. (2016). The influence of the Peroneus Longus muscle on the foot under axial loading: A CT evaluated dynamic cadaveric model study. *Clin Biomech, 34*, 7-11.

Fessel, G., Jacob, H.A.C., Wyss, C.H., Mittlmeier, T., Müller-Gerbl, M. and Büttner, A. (2014). Changes in length of the plantar aponeurosis during the stance phase of gait–an in vivo dynamic fluoroscopic study. *Ann Anat - Anat Anz, 196*(6), 471-478.

Gomes, M., Pinto, A.P., Fabián, A.A., Gomes, T.J.M., Navarro, A. and Oliva, X.M. (2019). Insertional anatomy of peroneal brevis and longus tendon—A cadaveric study. *Foot Ankle Surg, 25*(5), 636-639.

Hicks, J.H. (1954). The mechanics of the foot: II. The plantar aponeurosis and the arch. *J Anat, 88*(1), 25-30.

Hohmann, E., Keough, N., Glatt, V., Tetsworth, K., Putz, R. and Imhoff, A. (2019). The mechanical properties of fresh versus fresh/frozen and preserved (Thiel and Formalin) long head of biceps tendons: a cadaveric investigation. *Ann Anat, 221*, 186-191.

Hunt, A. and Smith, R. (2004). Mechanics and control of the flat versus normal foot during the stance phase of walking. *Clin Biomech*, *19*(4), 391-397.

Johnson, C. and Christensen, J. (1999). Biomechanics of the first ray part I. The effects of peroneus longus function: A three-dimensional kinematic study on a cadaver model. *J Foot Ankle Surg, 38*(5), 313-321.

Jones, R. (1941). The human foot. An experimental study of its mechanics, and the role of its muscles and ligaments in the support of the arch. *Am J Anat, 68*(1), 1-39.

Kaminski, T.W., Perrin, D.H. and Gansneder, B.M. (1999). Eversion strength analysis of uninjured and functionally unstable ankles. *J Athl Train*, 34(3), 239.

Kohls-Gatzoulis, J., Angel, J.C., Singh, D., Haddad, F., Livingstone, J. and Berry, G. (2004). Tibialis posterior dysfunction: a common and treatable cause of adult acquired flatfoot. *BMJ, 329*(7478), 1328-1333.

Konradsen, L., Voigt, M. and Hojsgaard, C. (1997). Ankle Inversion Injuries. *Am J Sports Med*, *25*(1), 54-58.

Moore, K., Agur, A. and Dalley, A. (2014). *Clinically oriented anatomy, Seventh Edition.* Lippincott Williams and Wilkins: Philadelphia.

Murley, G., Menz, H. and Landorf, K. (2009). Foot posture influences the electromyographic activity of selected lower limb muscles during gait. *J Foot Ankle Res*, *2*(1), 35.

Raj, M.A., DeCastro, A. and Kiel, J. (2019). Pes Planus. URL: https://www.ncbi.nlm.nih.gov/books/NBK430802/

Renton, P. (1991). *Radiology of the Foot. In: The Foot and its Disorders, L. Klenerman, editors, Third Edition*. Oxford: Blackwell Scientific, 259-346.

Schindelin, J., Arganda-Carreras, I., Frise, E., Kaynig, V., Longair, M., Pietzsch, T., Preibisch, S., Rueden, C., Saalfeld, S., Schmid, B. and Tinevez, J.Y. (2012). Fiji: an open-source platform for biological-image analysis. *Nat Methods, 9*(7), 676-682.

Sharkey, N., Ferris, L. and Donahue, S. (1998). Biomechanical Consequences of Plantar Fascial Release or Rupture During Gait: Part I - Disruptions in Longitudinal Arch Conformation. *Foot Ankle Int*, *19*(12), 812-820.

Shelton, T.J., Singh, S., Bent Robinson, E., Nardo, L., Escobedo, E., Jackson, L., Kreulen, C.D. and Giza, E. (2019). The Influence of Percentage Weight-Bearing on Foot Radiographs. *Foot*

*Ankle Spec, 12*(4), 363-369.

Standring, S. editor. (2005). Gray's Anatomy: The Anatomical Basis of Clinical Practice. *39th edition*. Elsevier Churchill Livingstone: Edinburgh.

Tao, X., Chen, W. and Tang, K. (2019). Surgical procedures for treatment of adult acquired flatfoot deformity: a network meta-analysis. *J Orthop Surg, 14*(1), 62.

Thordarson, D., Schmotzer, H., Chon, J. and Peters, J. (1995). Dynamic Support of the Human Longitudinal Arch. *Clin Orthop, 316*, 165-172.

Uchiyama, S., Coert, J.H., Berglund, L., Amadio, P.C. and An, K.N. (1995). Method for the measurement of friction between tendon and pulley. *J Orthop Res, 13*(1), 83-89.

Venkadesan, M., Yawar, A., Eng, C.M., Dias, M.A., Singh, D.K., Tommasini, S.M., Haims, A.H., Bandi, M.M. and Mandre, S. (2020). Stiffness of the human foot and evolution of the transverse arch. *Nature, 579*, 1-4.

Zhao, X., Tsujimoto, T., Kim, B., Katayama, Y. and Tanaka, K. (2018). Association of foot structure with the strength of muscles that move the ankle and physical performance. *J Foot Ankle Surg, 57*(6), 1143-1147.

## Footnotes

Footnote 1: Capstan equation: $\frac{T_1}{T_2} = e^{\mu\theta}$, where $T_1$ = tension proximal to directional change, $T_2$ = tension distal to directional change, $\mu$ = frictional coefficient, and $\theta$ = angle between line through the tendon prior to, and after the directional change.

## Conflicts of interest

The authors confirm no conflicts of interest.

## Figure Legends

**Figure 1a-d:** left foot.

(a) Lateral view. Origin of fibularis longus muscle and formation of its tendon (blue) posterior to lateral malleolus. Tendon passes deep to fibular retinaculum (red).

(b) Plantar view. Insertion of fibularis longus tendon, it passes deep to long plantar ligament (beige). $\theta$, angle of fibularis longus tendon on sole, measured between midline of foot (green line) and line passing through fibularis longus tendon (orange line).

(c) Plantar view. Placement of markers. (A) midpoint of calcaneus posteriorly, (B) medial aspect of medial cuneiform, (C) midpoint of base of fifth metatarsal. AB = longitudinal distance between markers (A) and (B), representing medial longitudinal arch. BC = transverse distance between markers (B) and (C), representing transverse arch.

(d) Plantar view. Deep dissection. Markers (pins) seen.

**Figure 2:** Experimental apparatus. Calcaneus clamped allowing access to fibularis longus tendon (blue). Laser level (yellow) used to align specimens. Photographs taken using iPad rested on platform above specimen.

**Figure 3:** left foot, lateral/plantar view. Capstan equation applied to fibularis longus tendon. $\frac{T_1}{T_3} = e^{\mu(\alpha+\beta)}$, where: $T_1$ = tension in fibularis longus tendon (blue) proximal to directional changes; $T_3$ = tension in fibularis longus tendon distal to directional changes; $\mu$ = frictional coefficient; $\alpha$ = angle of first directional change; $\beta$ = angle of second directional change.

**Figure 4:** Force-distance relationship of specimen 2, (a) BC transverse distance and (b) AB longitudinal distance. Plots are average of two repeats. $y_0$, predicted distance at force = 0; $y_{150}$, predicted distance at force = 150 N; B, asymptotic baseline distance when force = ∞; $\Delta_{dist150}$, predicted distance change caused by a force of 150 N, $\Delta_{dist150} = y_0 - y_{150}$.

**Figure 5:** Relationship between angle of fibularis longus tendon on sole (θ) and predicted distance change provided by a force of 150 N ($\Delta_{dist150}$) for both the transverse foot arch (TFA) and medial longitudinal arch (MLA). TFA: slope ± s.e. = 0.56 ± 0.13 mm.degree$^{-1}$, $r$ = 0.83, $p$ = 0.002; MLA: 0.18 ± 0.18 mm.degree$^{-1}$, $r$ = 0.32, $p$ = 0.33.

**Figure 1a-d**

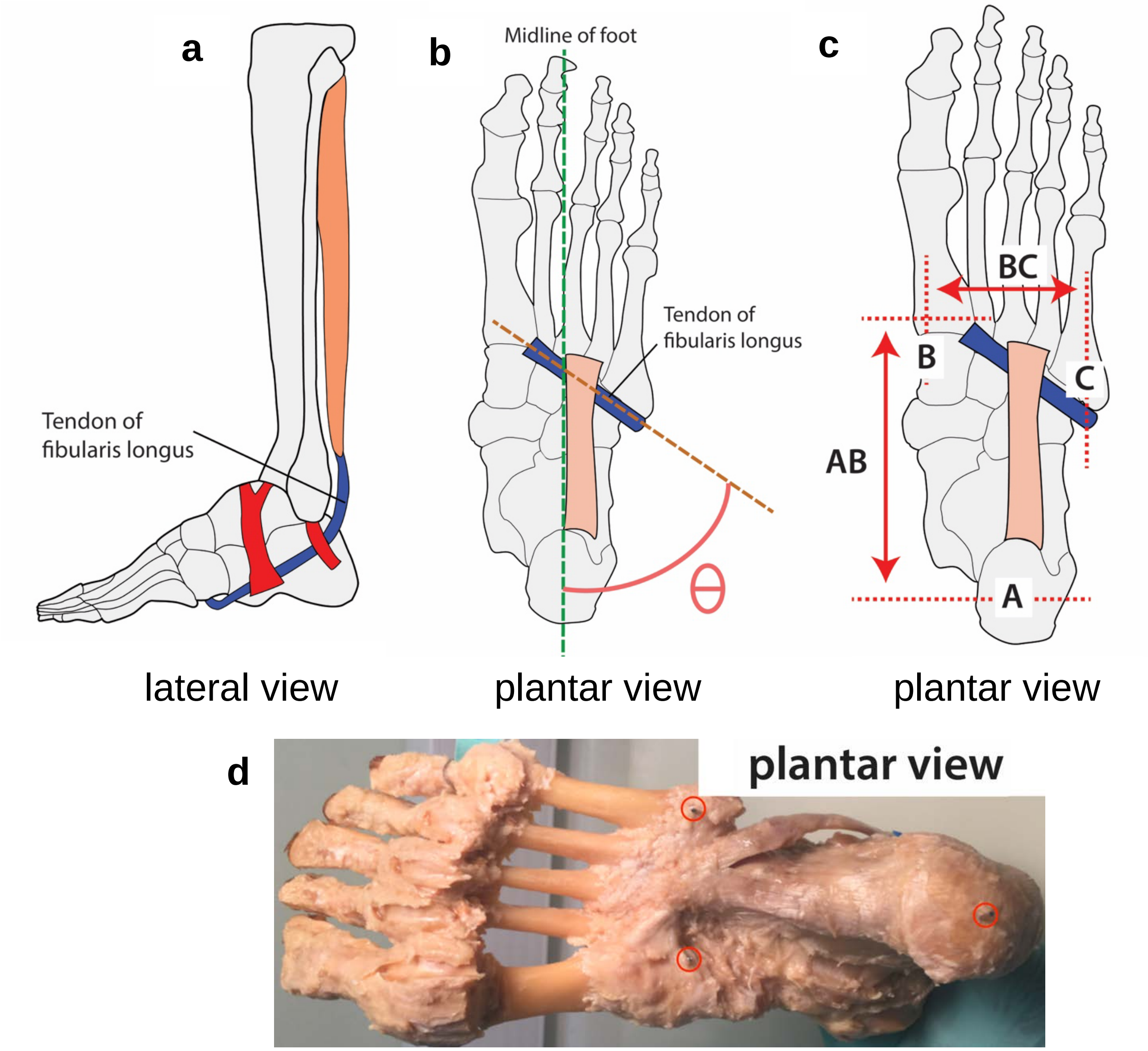
a
Tendon of fibularis longus
lateral view
b
Midline of foot
Tendon of fibularis longus
θ
plantar view
c
BC
B
C
AB
A
plantar view
d
plantar view

2 **Figure 2**

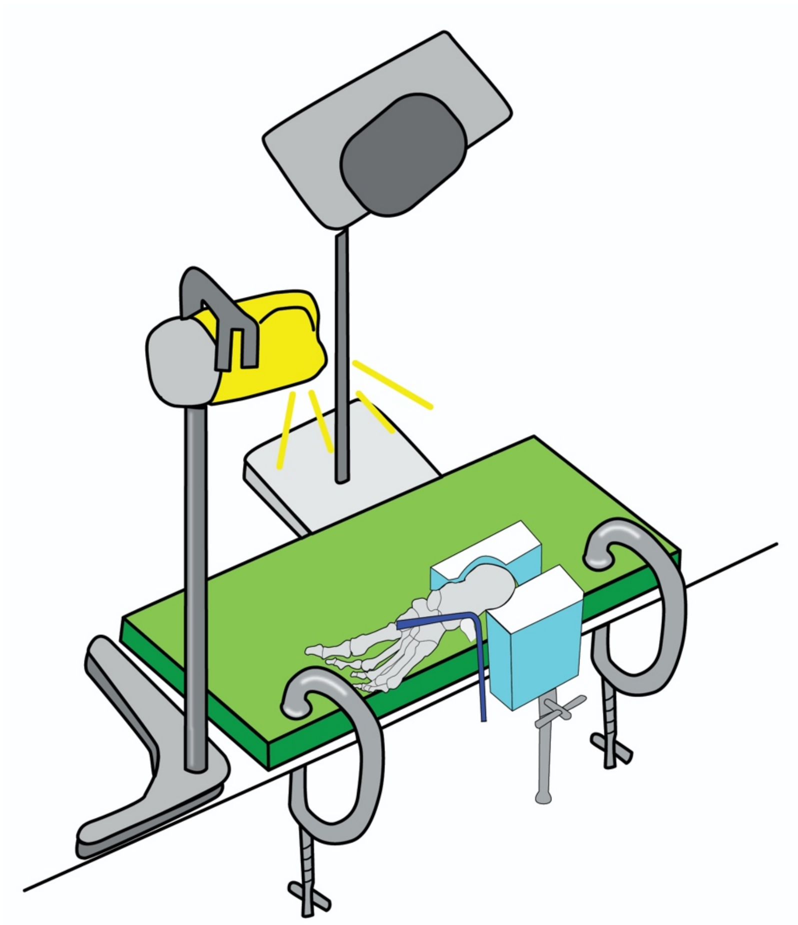

**Figure 3**

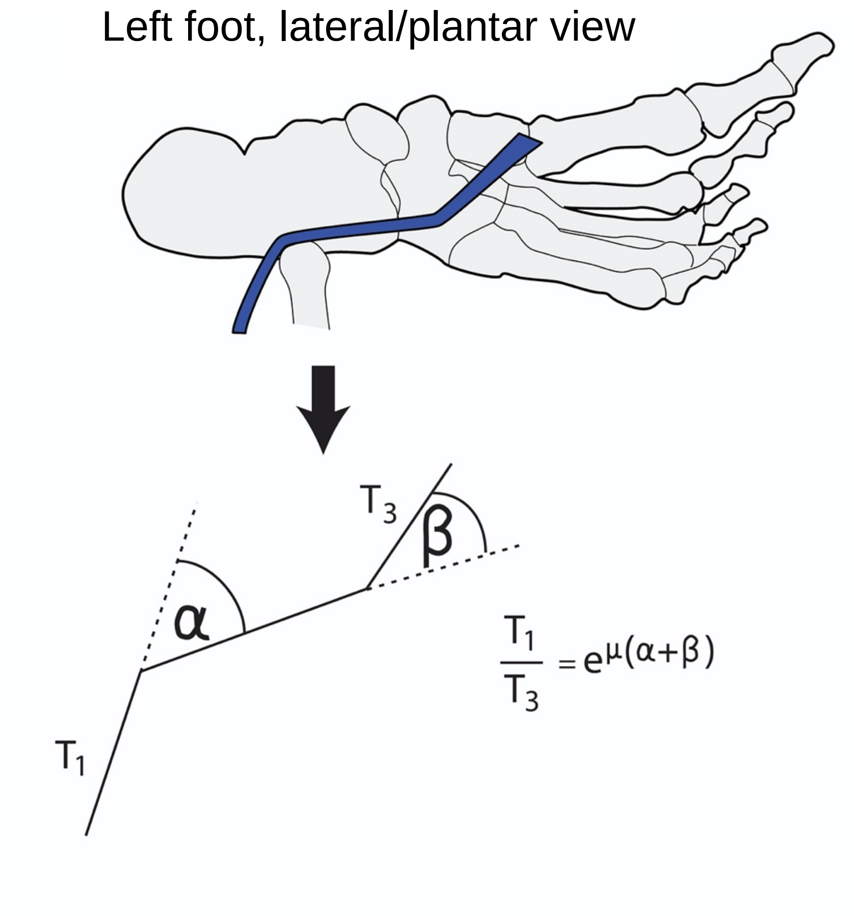
Left foot, lateral/plantar view
$T_3$
β
α
$T_1$
$\frac{T_1}{T_3} = e^{\mu(\alpha+\beta)}$

**Figure 4a-b**

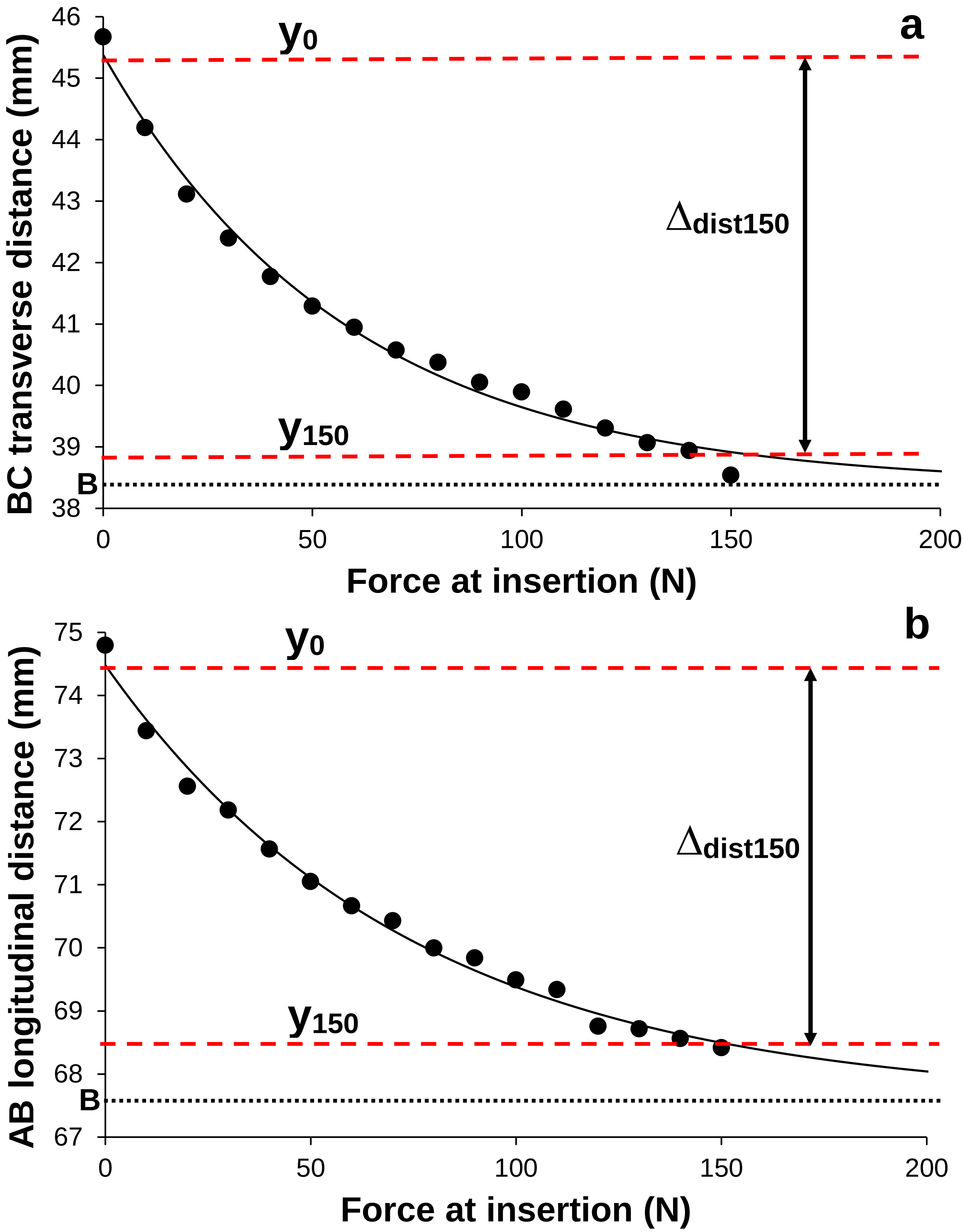

a
y0
y150
Δdist150
B
BC transverse distance (mm)
Force at insertion (N)
b
y0
y150
Δdist150
B
AB longitudinal distance (mm)
Force at insertion (N)

**Figure 5**

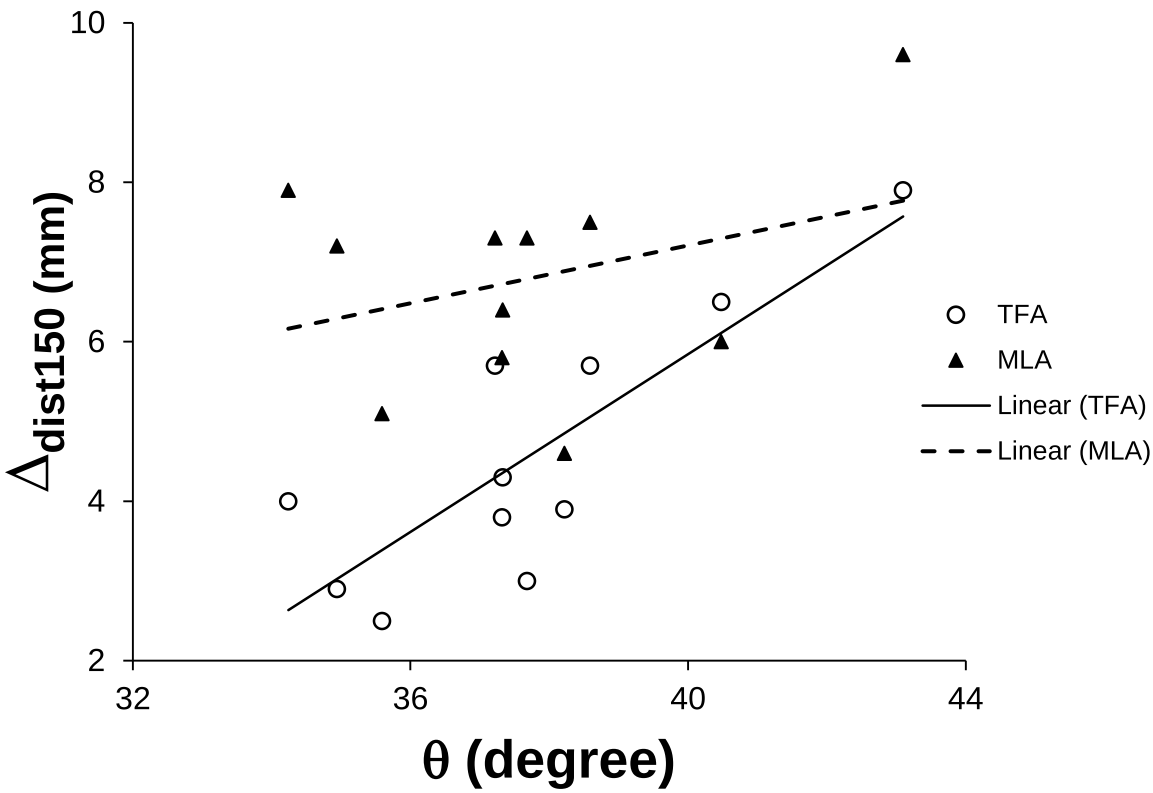

10
8
6
4
2
32
36
40
44
Δdist150 (mm)
θ (degree)
TFA
MLA
Linear (TFA)
Linear (MLA)

## 1 Tables

Table 1: Donor Characteristics and Parameter Estimates

| Specimen | Sex/Side | Age (years) | **θ (degrees)** | Transverse arch | | | | | Medial longitudinal arch | | | | |
|---|---|---|---|---|---|---|---|---|---|---|---|---|---|
| | | | | $y_0$ (mm) | B (mm) | k ($N^{-1}$) | **$\Delta_{dist150}$ (mm)** | CV (%) | $y_0$ (mm) | B (mm) | k ($N^{-1}$) | **$\Delta_{dist150}$ (mm)** | CV (%) |
| 1 | M/R | 68 | 37.68 | 45.5 | 40.8 | 0.0069 | 3.0 | 6.0% | 95.8 | 11.2 | 0.0006 | 7.3 | 1.5% |
| 2 | F/R | 84 | 40.48 | 45.4 | 38.4 | 0.017 | 6.5 | 9.1% | 74.5 | 67.6 | 0.013 | 6.0 | 3.1% |
| 3 | M/L | 62 | 43.10 | 42.6 | 32.1 | 0.0093 | 7.9 | 9.6% | 89.4 | 72.3 | 0.0055 | 9.6 | 4.3% |
| 4 | F/R | 74 | 37.33 | 42.7 | 35.2 | 0.0057 | 4.3 | 9.3% | 86.7 | 78.8 | 0.011 | 6.4 | 7.8% |
| 5 | M/L | 80 | 35.59 | 40.3 | 37.3 | 0.013 | 2.5 | 5.9% | 92.0 | 84.2 | 0.0071 | 5.1 | 10.0% |
| 6 | M/R | 55 | 38.22 | 38.2 | 31.9 | 0.0064 | 3.9 | 5.5% | 86.6 | 76.1 | 0.0038 | 4.6 | 15.4% |
| 7 | F/L | 86 | 34.94 | 39.8 | 35.6 | 0.0079 | 2.9 | 11.4% | 102.3 | 93.9 | 0.013 | 7.2 | 7.3% |
| 8 | M/R | 81 | 37.22 | 40.9 | 35.1 | 0.023 | 5.7 | 1.0% | 92.5 | 84.5 | 0.016 | 7.3 | 5.7% |
| 9 | F/R | 89 | 38.59 | 41.8 | 35.7 | 0.018 | 5.7 | 0.8% | 69.4 | 61.3 | 0.017 | 7.5 | 2.8% |
| 10 | F/R | 88 | 37.32 | 36.1 | 32.3 | 0.027 | 3.8 | 2.1% | 70.7 | 64.4 | 0.016 | 5.8 | 9.4% |
| 11 | F/L | 96 | 34.24 | 39.1 | 34.9 | 0.021 | 4.0 | 3.8% | 86.6 | 78.6 | 0.028 | 7.9 | 4.6% |
| **Mean** | - | 78.5 | **37.7** | 41.1 | 35.4 | 0.014 | **4.6** | 5.9% | 86.0 | 70.2 | 0.012 | **6.8** | 6.5% |
| **SD** | - | 12.5 | **2.5** | 2.9 | 2.7 | 0.0076 | **1.7** | 3.7% | 10.5 | 21.8 | 0.0077 | **1.4** | 4.0% |

Parameter estimates were obtained using the means of two replicate datasets. CV represents the coefficient of variation for $\Delta_{dist150}$ calculated from the two replicate measurements separately. Red indicates that the estimate from the second replicate is lower than the first and green that the estimate from the second is higher than the first. FL, fibularis longus; θ, angle of fibularis longus tendon on sole; B, asymptotic baseline distance when force = ∞; k, force constant defining relationship between force and distance; $\Delta_{dist150}$, predicted distance change between 0 and 150 N.

## Supplementary Tables

Table S-1: Mass (kg) applied to specimens

| Force (N) | Specimen 8, 9 | Specimen 2, 4, 5, 11 | Specimen 1, 3 | Specimen 6, 7, 10 |
|---|---|---|---|---|
| 0 | 0 | 0 | 0 | 0 |
| 10 | 1.08 | 1.08 | 1.08 | 1.09 |
| 20 | 2.15 | 2.16 | 2.16 | 2.17 |
| 30 | 3.23 | 3.24 | 3.25 | 3.26 |
| 40 | 4.30 | 4.31 | 4.33 | 4.34 |
| 50 | 5.38 | 5.39 | 5.41 | 5.43 |
| 60 | 6.45 | 6.47 | 6.49 | 6.51 |
| 70 | 7.53 | 7.55 | 7.57 | 7.60 |
| 80 | 8.60 | 8.63 | 8.66 | 8.68 |
| 90 | 9.68 | 9.71 | 9.74 | 9.77 |
| 100 | 10.75 | 10.79 | 10.82 | 10.85 |
| 110 | 11.83 | 11.86 | 11.90 | 11.94 |
| 120 | 12.90 | 12.94 | 12.98 | 13.02 |
| 130 | 13.98 | 14.02 | 14.07 | 14.11 |
| 140 | 15.05 | 15.10 | 15.15 | 15.19 |
| 150 | 16.13 | 16.18 | 16.23 | 16.28 |

Specimens numbered corresponding to order in Table 1. Mass calculated using Capstan equation. Directional change of fibularis longus tendon at the lateral malleolus fixed at 47.5 degrees. Directional change of fibularis longus tendon as it crosses from the lateral aspect of the foot onto the sole was 40 (specimens 8, 9), 45 (specimens 2, 4, 5, 11), 50 (specimens 1, 3), 55 (specimens 6, 7, 10) degrees.

4

Table S-2: BC transverse distance (mm)

| Force (N) | 1 | | 2 | | 3 | | 4 | | 5 | | 6 | | 7 | | 8 | | 9 | | 10 | | 11 | |
|---|---|---|---|---|---|---|---|---|---|---|---|---|---|---|---|---|---|---|---|---|---|---|
| 0 | 45.09 | 45.57 | 46.23 | 45.11 | 43.15 | 41.59 | 42.76 | 42.50 | 40.52 | 40.14 | 38.58 | 37.77 | 39.94 | 39.34 | 41.64 | 41.08 | 42.24 | 42.35 | 36.39 | 36.34 | 39.82 | 39.11 |
| 10 | 45.03 | 45.41 | 44.35 | 44.04 | 42.50 | 41.19 | 42.16 | 42.38 | 40.37 | 39.74 | 38.14 | 37.56 | 39.64 | 39.25 | 39.55 | 39.09 | 40.49 | 40.34 | 35.22 | 34.89 | 38.30 | 37.46 |
| 20 | 44.73 | 45.06 | 43.34 | 42.88 | 41.35 | 40.66 | 41.55 | 41.92 | 39.61 | 39.05 | 37.43 | 37.41 | 39.43 | 39.15 | 38.61 | 38.38 | 39.60 | 39.49 | 34.11 | 34.03 | 37.77 | 37.01 |
| 30 | 44.24 | 44.91 | 42.74 | 42.05 | 40.53 | 39.63 | 41.47 | 41.64 | 39.50 | 39.01 | 36.96 | 36.79 | 39.38 | 38.71 | 38.10 | 37.56 | 39.48 | 38.81 | 33.79 | 33.82 | 37.38 | 36.92 |
| 40 | 43.95 | 44.81 | 42.05 | 41.49 | 39.94 | 38.67 | 41.38 | 41.24 | 39.14 | 38.88 | 36.92 | 36.74 | 39.01 | 38.44 | 37.61 | 37.27 | 39.12 | 38.72 | 33.51 | 33.45 | 37.28 | 36.06 |
| 50 | 43.76 | 44.38 | 41.52 | 41.06 | 39.08 | 38.32 | 40.83 | 40.97 | 39.14 | 38.65 | 36.76 | 36.01 | 38.66 | 38.21 | 37.48 | 36.93 | 38.11 | 38.17 | 33.48 | 33.42 | 36.99 | 36.03 |
| 60 | 43.59 | 44.11 | 41.02 | 40.87 | 38.17 | 37.55 | 40.49 | 40.17 | 38.89 | 38.33 | 36.54 | 35.92 | 38.57 | 37.97 | 37.10 | 36.51 | 38.10 | 37.64 | 33.28 | 33.25 | 36.52 | 35.83 |
| 70 | 43.51 | 43.96 | 40.55 | 40.60 | 38.12 | 36.96 | 40.41 | 39.83 | 38.81 | 38.28 | 35.96 | 35.76 | 38.12 | 37.63 | 36.70 | 35.86 | 37.68 | 37.61 | 32.93 | 32.87 | 36.34 | 35.71 |
| 80 | 43.22 | 43.54 | 40.45 | 40.30 | 37.50 | 36.53 | 40.11 | 39.61 | 38.73 | 38.10 | 36.06 | 35.42 | 38.07 | 37.54 | 36.24 | 35.84 | 37.52 | 37.16 | 32.87 | 32.84 | 36.03 | 35.40 |
| 90 | 43.15 | 43.50 | 40.15 | 39.95 | 37.12 | 36.38 | 39.87 | 39.45 | 38.68 | 37.96 | 35.79 | 35.31 | 37.54 | 37.50 | 36.08 | 35.75 | 37.30 | 36.94 | 32.78 | 32.59 | 35.70 | 35.36 |
| 100 | 42.57 | 43.17 | 39.95 | 39.84 | 36.43 | 35.84 | 39.53 | 39.41 | 38.39 | 37.91 | 35.75 | 34.93 | 37.57 | 37.34 | 35.98 | 35.37 | 36.77 | 36.71 | 32.70 | 32.58 | 35.67 | 35.12 |
| 110 | 42.60 | 43.38 | 39.72 | 39.50 | 36.12 | 35.54 | 39.49 | 39.20 | 38.22 | 38.00 | 35.36 | 34.35 | 37.44 | 37.12 | 35.69 | 35.69 | 36.61 | 36.63 | 32.46 | 32.50 | 35.50 | 34.85 |
| 120 | 42.66 | 43.13 | 39.23 | 39.38 | 35.57 | 35.36 | 39.00 | 39.06 | 37.93 | 37.93 | 34.96 | 34.33 | 37.28 | 37.11 | 35.65 | 35.29 | 36.54 | 36.44 | 32.44 | 32.47 | 35.47 | 34.81 |
| 130 | 42.59 | 42.55 | 39.01 | 39.12 | 35.18 | 35.28 | 38.92 | 38.48 | 37.93 | 37.63 | 34.88 | 34.23 | 37.23 | 37.07 | 35.57 | 35.03 | 36.42 | 36.13 | 32.28 | 32.27 | 35.47 | 34.81 |
| 140 | 42.57 | 42.62 | 38.94 | 38.94 | 35.04 | 35.12 | 38.77 | 38.24 | 37.79 | 37.64 | 34.75 | 34.15 | 37.05 | 37.00 | 35.37 | 34.97 | 36.03 | 36.03 | 32.24 | 32.13 | 35.27 | 34.87 |
| 150 | 42.35 | 42.61 | 38.76 | 38.32 | 35.02 | 34.17 | 38.65 | 38.19 | 37.84 | 37.50 | 34.73 | 34.09 | 36.96 | 36.96 | 35.11 | 34.98 | 35.93 | 35.89 | 32.01 | 32.04 | 35.36 | 34.76 |

Specimens ordered corresponding to order in Table 1. Two repeats per specimen.

5

Table S-3: AB longitudinal distance (cm)

| Force (N) | 1 | | 2 | | 3 | | 4 | | 5 | | 6 | | 7 | | 8 | | 9 | | 10 | | 11 | |
|---|---|---|---|---|---|---|---|---|---|---|---|---|---|---|---|---|---|---|---|---|---|---|
| 0 | 95.09 | 95.90 | 75.03 | 74.56 | 88.51 | 89.38 | 87.23 | 86.95 | 92.44 | 92.05 | 86.91 | 86.85 | 102.19 | 102.05 | 93.92 | 92.74 | 70.26 | 69.94 | 71.23 | 70.65 | 86.90 | 86.77 |
| 10 | 94.05 | 95.77 | 74.02 | 72.86 | 88.26 | 89.08 | 86.12 | 85.27 | 91.54 | 91.01 | 86.06 | 86.38 | 102.05 | 100.94 | 91.31 | 90.47 | 67.67 | 67.73 | 69.94 | 68.91 | 84.55 | 84.76 |
| 20 | 94.08 | 95.88 | 73.01 | 72.11 | 87.50 | 88.47 | 85.20 | 84.54 | 91.21 | 90.43 | 85.60 | 85.27 | 100.60 | 100.10 | 90.48 | 89.09 | 66.67 | 66.42 | 69.05 | 68.49 | 82.59 | 82.68 |
| 30 | 93.50 | 95.09 | 72.48 | 71.88 | 86.45 | 87.26 | 84.10 | 84.09 | 90.99 | 89.89 | 85.45 | 85.06 | 100.17 | 99.14 | 89.60 | 88.67 | 66.07 | 65.59 | 68.58 | 67.70 | 82.35 | 81.50 |
| 40 | 92.46 | 94.93 | 71.84 | 71.29 | 86.26 | 86.19 | 83.91 | 83.62 | 90.45 | 89.60 | 84.96 | 84.84 | 99.51 | 98.44 | 88.56 | 88.22 | 65.83 | 65.00 | 68.15 | 67.51 | 81.29 | 80.98 |
| 50 | 92.57 | 93.96 | 71.52 | 70.58 | 85.43 | 85.89 | 83.49 | 83.16 | 90.00 | 89.07 | 84.75 | 84.64 | 98.72 | 97.83 | 88.41 | 87.67 | 64.82 | 64.40 | 67.32 | 66.79 | 80.57 | 80.49 |
| 60 | 92.41 | 93.72 | 71.02 | 70.31 | 84.57 | 85.29 | 83.07 | 82.83 | 89.68 | 88.88 | 84.32 | 84.38 | 97.83 | 97.40 | 88.13 | 87.35 | 64.70 | 64.08 | 67.02 | 66.49 | 80.40 | 80.09 |
| 70 | 92.10 | 93.30 | 70.77 | 70.08 | 83.31 | 84.07 | 82.51 | 82.39 | 89.43 | 88.53 | 84.08 | 84.17 | 97.19 | 96.80 | 87.56 | 86.85 | 64.22 | 63.66 | 66.42 | 66.06 | 80.30 | 79.99 |
| 80 | 91.46 | 92.98 | 70.52 | 69.47 | 83.31 | 83.09 | 82.32 | 82.01 | 89.31 | 88.23 | 83.81 | 84.00 | 97.13 | 96.56 | 87.46 | 86.82 | 64.18 | 63.39 | 66.03 | 66.02 | 80.06 | 79.29 |
| 90 | 91.19 | 92.89 | 70.43 | 69.25 | 82.46 | 82.79 | 81.84 | 81.72 | 88.78 | 88.10 | 83.65 | 83.75 | 96.88 | 96.10 | 87.27 | 86.61 | 63.53 | 63.07 | 65.95 | 65.72 | 79.60 | 79.06 |
| 100 | 89.52 | 91.78 | 69.84 | 69.14 | 81.28 | 82.17 | 81.49 | 81.60 | 88.62 | 87.76 | 83.39 | 83.44 | 96.73 | 95.97 | 86.93 | 86.19 | 63.02 | 62.54 | 65.91 | 65.68 | 79.35 | 78.96 |
| 110 | 88.85 | 91.79 | 69.63 | 69.04 | 81.38 | 82.04 | 81.21 | 81.29 | 87.76 | 87.56 | 82.65 | 83.39 | 95.98 | 95.82 | 86.28 | 85.60 | 62.87 | 62.54 | 65.63 | 65.54 | 79.24 | 78.93 |
| 120 | 88.76 | 89.60 | 68.86 | 68.65 | 80.66 | 81.12 | 80.93 | 80.93 | 87.33 | 87.47 | 82.43 | 82.99 | 95.82 | 95.76 | 86.06 | 85.34 | 62.74 | 62.35 | 65.57 | 65.35 | 79.15 | 78.60 |
| 130 | 88.39 | 90.14 | 68.82 | 68.61 | 80.05 | 80.83 | 80.55 | 80.69 | 87.18 | 87.40 | 82.05 | 82.68 | 95.18 | 95.62 | 85.79 | 85.09 | 62.26 | 61.85 | 65.44 | 65.09 | 78.87 | 78.45 |
| 140 | 88.30 | 89.54 | 68.76 | 68.36 | 80.45 | 80.70 | 80.29 | 80.57 | 87.01 | 87.30 | 81.73 | 82.66 | 95.04 | 95.49 | 85.14 | 84.77 | 61.99 | 61.42 | 64.74 | 64.71 | 78.75 | 78.39 |
| 150 | 88.09 | 88.71 | 68.71 | 68.12 | 80.33 | 79.92 | 79.99 | 79.98 | 86.81 | 86.74 | 81.38 | 82.28 | 94.98 | 95.12 | 84.94 | 84.50 | 61.57 | 61.37 | 64.63 | 64.66 | 78.60 | 78.15 |

Specimens ordered corresponding to order in Table 1. Two repeats per specimen.